Exozodiacal Disk Detection Potential with the Keck Interferometer

E. Serabyn, M. M. Colavita and C. A. Beichman

Jet Propulsion Laboratory 171-113, 4800 Oak Grove Drive, Pasadena, CA 91109, USA

Abstract. If the dust content of nearby solar systems is comparable to, or larger than, that of our own zodiacal disk, the thermal emission from "exozodiacal" disks will significantly outshine planetary companions to nearby stars. As such, the characterization of flux levels from exozodiacal disks is a vital first step on the road to direct planet detection. To this end, a nulling interferometry mode is being implemented on the forthcoming Keck Interferometer. By interferometrically nulling out the mid-infrared radiation from the central star, attendant thermal emission from exozodiacal dust will be rendered more readily detectable. In the following, we estimate the sensitivity of the Keck nulling interferometer to exozodiacal dust emission.

1. Introduction

The large brightness contrast between stellar emission and attendant planetary and exozodiacal dust emission sources can be significantly reduced with the novel observational technique of achromatic nulling interferometry (Shao & Colavita 1992, Woolf & Angel 1998). In this approach, broadband destructive interference of the starlight collected by two telescope apertures is enlisted to reject the on-axis stellar signal, leaving off-axis planetary and exozodiacal emission much more amenable to detection. As thermal emission from planets and exozodiacal dust at temperatures of a few hundred degrees Kelvin peaks in the mid-infrared (MIR), the contrast ratio is significantly better in the MIR than at optical wavelengths. Nascent nulling experiments are therefore targeting the 10 micron region of the spectrum, where the terrestrial atmosphere fortuitously has a favorable transmission window (from 8 to 13.5 μm).

If our solar system were observed from a distance of 10 pc, its 10 μm emission would be dominated by a stellar flux of 2.2 Jy. Next in brightness, about 4 orders of magnitude dimmer, would be the thermal emission arising from our solar system's zodiacal dust disk (Traub, Carleton & Angel 1996, Angel 1998, Beichman, Woolf & Lindensmith 1999). (Significant uncertainty attends the zodiacal estimate due to the need to extrapolate local MIR measurement inward to several solar radii). As to the planets, Jupiter's emission would be yet another two orders of magnitude fainter, at about 2 μJy, while the Earth would show up with a mere 0.25 μJy. Thus, extrapolating from our own solar system, the brightest non-stellar MIR emission from nearby solar systems may arise in comparable "exozodiacal" dust disks, thus providing a second (after the star itself)

significant hindrance to the direct imaging of nearby planets. Indeed, IRAS and ISO observations probe only to the few hundred solar-zodiacal equivalent (hereafter abbreviated "zodi") level. Recognizing this, one of the key goals of NASA's Keck Interferometer project is the detection and characterization of exozodiacal emission around nearby stars, as a prelude to the proposed Terrestrial Planet Finder (TPF) mission (Beichman, Woolf & Lindensmith 1999), which would subsequently look for the planets themselves. Here we present signal-to-noise ratio (SNR) estimates for the detectability of faint exozodiacal emission with the Keck Interferometer.

2. Single Aperture Sensitivities

With currently available MIR cameras, the detection of an isolated mJy-level source at a wavelength, λ, of 10 μm, is not overly difficult for a large-aperture telescope at a high, dry site. Although published sensitivities depend on the specific camera used, the radiation passband, and the seeing (or beamsize), extant MIR cameras used to date on the Keck telescopes typically show noise equivalent powers of order 10 mJy/Hz$^{0.5}$ per beam (http://astro.caltech.edu/mirror/keck/realpublic/inst/). A single-aperture SNR of order unity is thus achievable on an (isolated) 50 zodi signal in an observation time of 1 second. In the absence of a much brighter stellar companion, the theoretical single-aperture sensitivity limit for one night of observation is then of order 1 zodi.

Simple ground-based photometric sensitivities would thus be sufficient to probe exozodiacal disks to much fainter levels than was possible with either the IRAS or ISO satellites, if the disks were not located near very bright stellar sources. The main issues to be faced by a ground-based nulling experiment are therefore not related to sensitivity, but to the rejection of the much brighter emission from both the central star (brighter by 2 to 4 orders of magnitude for flux levels of 100 to 1 zodi), and the even brighter thermal background radiation from the sky (brighter by 4 to 6 orders of magnitude for 100 to 1 zodis).

3. Experimental Overview

In the discussion of the experimental architecture which follows, we generally confine ourselves to the highest level optical layout, except for our throughput estimates, where a full acounting of losses is essential. A more complete discussion can be found at http://www.jpl.nasa.gov. The basic experimental architecture begins with the two Keck telescopes, which transmit the light they collect to a beam combining laboratory in the basement of the Keck observatory. Adaptive optics wavefront correction immediately after the telescopes provides a corrected beam with a Strehl ratio exceeding 98.5% at $\lambda = 10$ μm. (This level is required to assure an intensity match between the two apertures sufficient to allow precise cancellation of the two incoming on-axis electric fields). Thus, in the MIR, each Keck aperture will in essence provide a nearly perfectly corrected beam, with a point spread function (PSF) core of FWHM $\approx 0.2''$. By coupling this PSF core to a detector through a single-mode spatial filter (Shao & Colavita 1992), the interferometer will be sensitive only to radiation within a single telescope diffraction beam. The sensitivity of the Keck Interferometer to

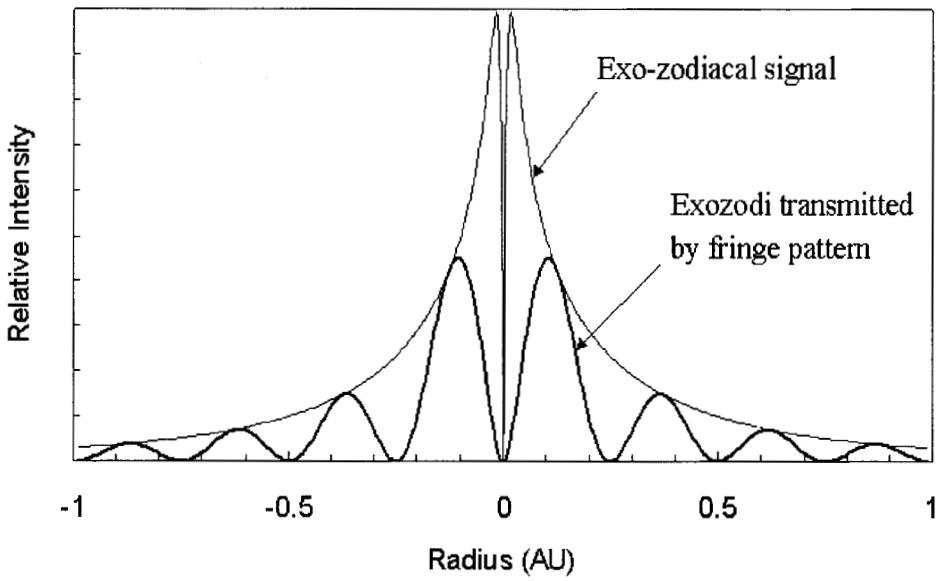

Figure 1. Cross-section through an exozodiacal disk along the direction of the fringe pattern. The top curve shows the intrinsic exozodiacal emission, and the bottom curve gives the intensity transmitted by the nulling interferometer.

exozodiacal emission will thus be limited to a radial extent of about a tenth of an arc second around the star, and so for stars at distances, d, in the range 1 to 10 pc, the Keck PSF core will couple to exozodiacal emission arising interior to radii of 0.1 AU to 1 AU. Thus, sensitivity to the bulk of an exozodiacal disk comparable to our own (2-3 AU in outer radius, with a steep profile and sharp central peak (Fig. 1) is only obtained for distances as large as 10 pc.

Next we consider the effect of interferometrically combining the light collected by the two telescope apertures. As usual (Thompson, Moran & Swenson 1986), the result of interfering the two beams is to introduce sine-squared responsivity fringes across the far-field, because in the small angle approximation, the relative delay between the two apertures depends linearly on the off-axis field angle. As each additional wavelength of relative delay adds a fringe, the angular spacing of the fringes on the sky is $\lambda/B_{\rm p}$, where $B_{\rm p}$ is the projected baseline between the two apertures. For the Keck baseline of 85 m (8.5 times the aperture size), and incidence angles of 0° to 45°, the number of fringes crossing the single-aperture PSF core will then lie in the range 6 to 8.5 (Fig. 1). As AU-sized disks will be extended on the scale of the PSF core, roughly half of the exozodiacal signal will be transmitted by the interferometer's fringe response pattern at any given time (Fig 1).

The basic idea of achromatic nulling interferometry is then to combine the beams such that a broadband destructive interference fringe is placed on top of the star, thus removing this component of the incoming flux. Very important to this approach is that the nulling of the central star be carried out achromatically,

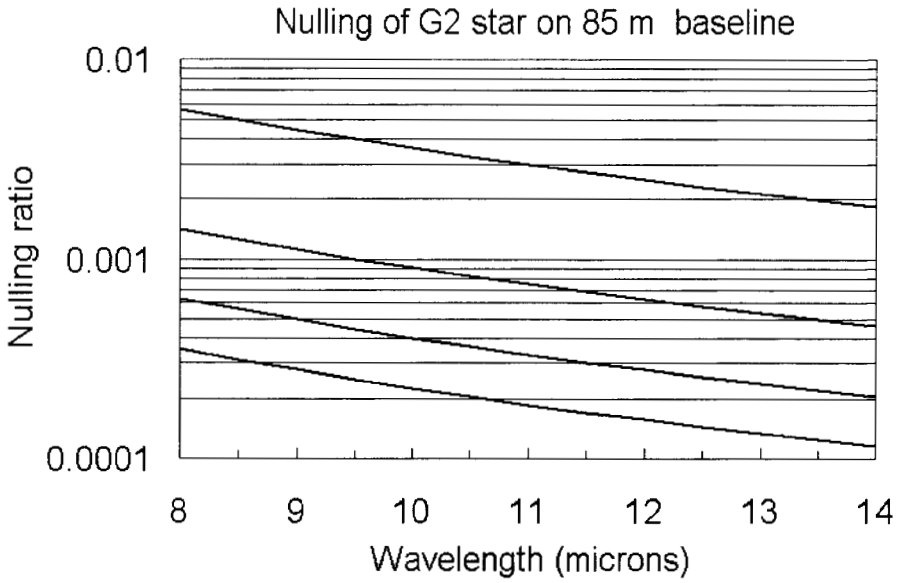

Figure 2. Theoretical stellar nulling ratio on the 85 m Keck baseline for G2 stars located at distances of 5, 10, 15 and 20 pc (top to bottom).

allowing simultaneous rejection of the stellar signal at all wavelengths. The approach to be used in the Keck interferometer is the introduction of a geometric flip between the electric fields from the two telescopes by means of a rotational shearing interferometer (Shao & Colavita 1992), so that at zero optical path difference, deep achromatic cancellation can occur.

How deep can the stellar cancellation be? Symmetry and stability are of course major practical limitations, but one fundamental limit cannot be overcome: the finite stellar diameter provides off-axis light which can leak around even a perfect on-axis null fringe. For a finite stellar diameter, the central null depth, N, (the ratio of destructive to constructive transmissions) at any λ is given by

$$N = \left(\frac{\pi}{4}\frac{\theta_*}{\lambda/B_\mathrm{p}}\right)^2 = \left(\frac{\pi}{4}\frac{B_\mathrm{p}}{\lambda}\frac{D_*}{d}\right)^2 \quad (1),$$

where θ_* and D_* are the angular and linear stellar diameters, respectively. As can be seen from Eqn. 1, the null depth improves as the inverse square of the stellar distance. For solar-type stars ($\theta_* = 9.3/d$ mas), and the 85 m Keck baseline, a null depth of a part in 1000 is attainable at $\lambda = 10$ μm for stars at $d \geq 10$ pc (Fig. 2). Deep stellar nulling and good coupling to AU-sized exozodiacal disks thus both call for target stars located at $d \geq 10$ pc. Leaving aside questions of SNR and nonidealities, the stellar flux can then be reduced to the 1 to 10 zodi range for G2 stars in the 33 - 10 pc range.

As can be seen from Eq. 1, the broader fringes at long wavelengths provide for a more favorable stellar rejection. In particular, Fig. 2 shows that for stars at $d = 10$ pc, the stellar rejection ratio for normal incidence on the 85 m Keck

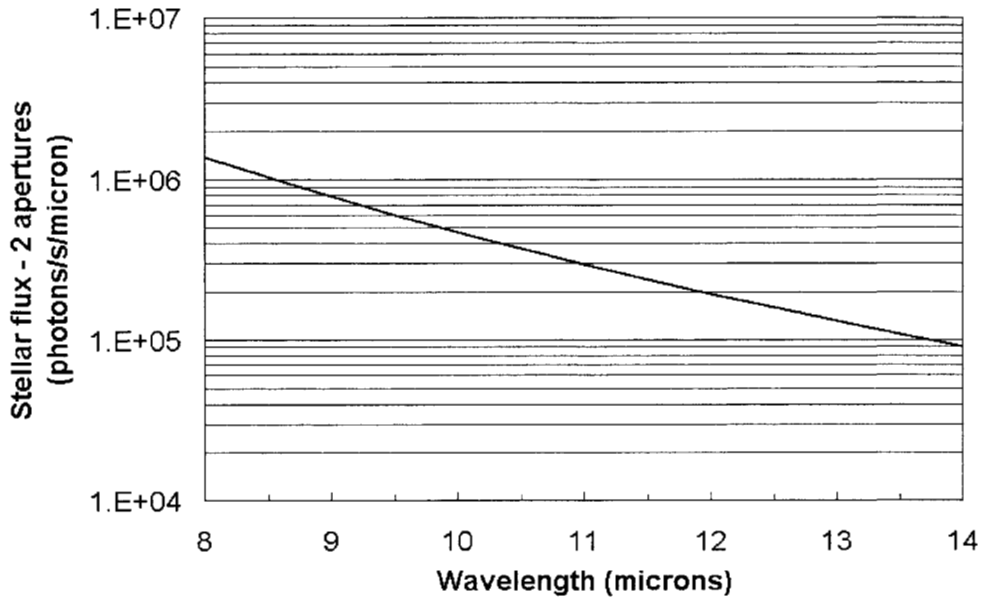

Figure 3. Stellar photon flux per micron transmitted by an ideal Keck interferometer null fringe. The calculations assume a G2 star at 10 pc, and 10 m apertures. The detected photon flux is lower by the net throughput given in Table 1.

baseline will vary from a part in 2000 at 13.5 microns to a part in 700 at 8 microns. For incidence at 45 degrees, foreshortening of the baseline improves the null depth by a factor of 2 (roughly equivalent to the 15 pc curve in Fig. 2). However, the transmitted stellar spectrum rises even more steeply to short wavelengths (Fig. 3), because of the incident spectrum's near Rayleigh-Jeans dependence in the MIR. Specifically, in the Rayleigh-Jeans limit, the ideal (i.e., lossless) nulled dual-aperture photon arrival rate per micron, $R_{\lambda,s}$, increases as the fifth power of the frequency, as can be seen from

$$R_{\lambda,s}(\text{photons/s/}\mu\text{m}) = \frac{\pi^4 k}{64h}\frac{T_*\theta_*^4}{\lambda^5}B_{\text{p}}^2 D_{\text{t}}^2\Big(\frac{x}{e^x-1}\Big), \tag{2}$$

where k is Boltzmann's constant, T_* is the stellar temperature, h is Planck's constant, D_t is the telescope diameter, and $x = h\nu/kT_*$. For stars of solar temperature, the last factor in parenthesis is within 15% of unity across the band, implying that most of the wavelength-dependence is contained in the λ^{-5} factor. This conclusion provides a very strong impetus for operation at the longest possible MIR wavelengths, where at the same time the exozodiacal/stellar contrast ratio is also optimized. However, as the thermal background flux increases to long wavelengths, the situation is really not quite so transparent. We thus turn to a discussion of the background flux.

4. Thermal Background

In essence, nulling removes the stellar signal, leaving the exozodiacal emission exposed. However, as in all MIR astronomical observations, the signal of interest must then be detected in the presence of a large thermal background. In principle, the background emission can be removed by employing spatial chopping, or by interferometric pathlength modulation. Leaving aside the optical details, here we aim our discussion toward an estimation of the achievable SNR, and assume that modulation results in a standard factor of 2 SNR degradation.

To estimate the background level associated with the Keck interferometer, a few further details concerning the optical system are necessary. As already indicated, the two Keck apertures are followed by an adaptive optics system. Thereafter, a series of transport mirrors carry the two beams to the basement of the Keck observatory, where a pair of optical delay lines (fast and slow) equalizes paths to the source, before the beams are combined in a cryogenic nulling beam combiner, or NBC. Finally, a cryogenic MIR camera with an Si:As detector array senses the light after its passage through a single-mode spatial filter.

Due to the extended nature of the optical train, and the independent functions performed by the various optical subsystems (such as wavefront correction, beam transport, slow and fast pathlength equalization, and beam compression), the number of room-temperature optical elements in the beam train is sizeable. Prior to entering the cryogenic NBC environment, roughly 30 mirror reflections take place, along with three ZnSe window transmissions, one dichroic beamsplitter reflection, and one beamsplitter transmission. The net result of passage down the optical train is thus a fairly substantial buildup of thermal emission. However, due to reabsorption in the optical train, for a series of n mirrors of identical emissivity $\epsilon_{\rm m}$, the net emissivity, ϵ_n, is not quite as large as a simple emissivity summation over the mirror train ($n\epsilon_{\rm m}$) would imply. Instead, the net emissivity is given by

$$\epsilon_n = 1 - (1 - \epsilon_{\rm m})^n \tag{3}$$

which in the second order approximation is fractionally smaller than $n\epsilon_{\rm m}$ by a factor of about $n\epsilon_{\rm m}/2$, or 20 to 33% for $n = 30$ and $\epsilon_{\rm m} = 1.5\%$ to 3%.

Of course, the net emissivity includes other sources, such as e.g. diffractive spillover and window and beamsplitter lossess, and so a complete emissivity accounting was undertaken. Under the assumptions of 98.5% reflection for clean mirror surfaces, 97% for dirty mirrors, 0.5% reflection losses at window surfaces, 0.5 to 1% window transmission losses, 5% beamsplitter losses, a coupling efficiency to the single-mode filter (pinhole) of 70% , and 12 % warm diffractive spillover from the cold aperture stop, the net emissivity of the warm optical train is expected (Table 1) to be of order 53% for "clean" optics, and 65% for "dirty" optics. These two cases form the starting point for two limiting estimates considered in the following, referred to hereafter as the "optimistic" and "pessimistic" cases. Where other parameters possess substantial uncertainty ranges, such as e.g. detective quantum efficiency, the relevant uncertainties are also folded into the two cases. The net result of our detailed transmission/emission budget for the optical train is given in Table 1, wherein a factor of 3 is seen to separate the throughputs in the optimistic and pessimistic cases. The net detected emis-

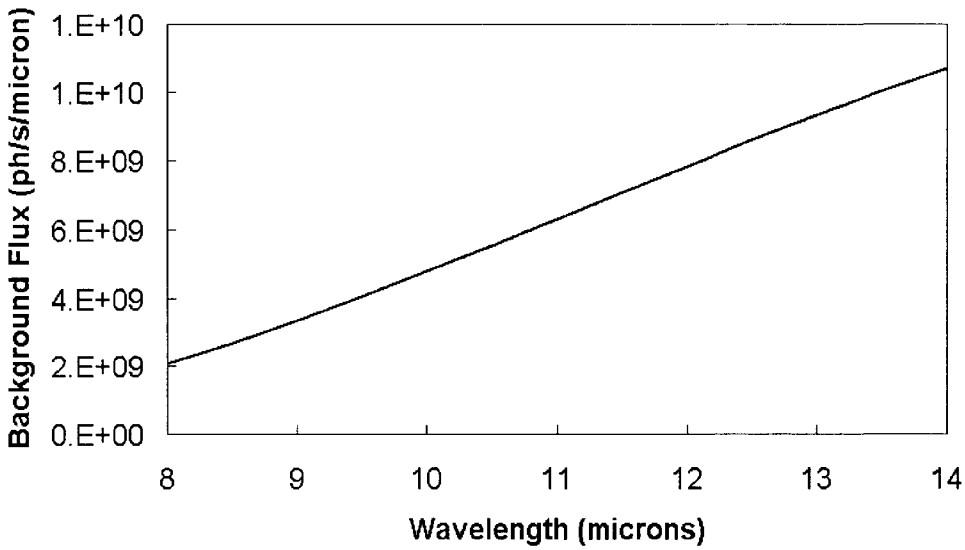

Figure 4. Detected background flux per micron for $T_b = 10$ C and a net detected emissivity of 13%.

sivities (Table 1) differ by a much smaller factor, both because of transmission losses occuring at cold (non-emissive) elements, and diffraction effects.

Given a cold throughput, t_c in the range 14 - 33%, the detected background comprises roughly 9 - 17 % of the background photon arrival rate in a single spatial mode, given by

$$R_{\lambda,b}(\text{photons/s/}\mu\text{m}) = t_c \frac{2kT_b}{h\lambda} \frac{x}{e^x - 1}, \tag{4}$$

where T_b is the background temperature. The detected background flux for the average of the two cases considered is plotted in Fig. 4. Comparing figs. 3 and 4, it can be seen that the shot noise in 1 second in a 30roughly 15 - 30 zodis (allowing for modulation). This is about a factor of two better than the single-aperture estimate of Section 2. Evidently the confinement of both the signal and the background to a single spatial mode (the adaptive optics system concentrates the stellar light signal, while the single-mode filter limits eliminates the background beyond the single transmitted spatial mode) compensates for the higher emissivity introduced by the long beam train. However, it must be borne in mind that the comparison is somewhat unfair - measured numbers on real cameras on the one hand, vs. performance expectations on the other.

Table 1. Throughput and Emissivity of the Keck Interferometer Optics

	Pessimistic Case	Optimistic Case
Warm Transmission	0.32	0.43
Cold Transmision	0.36	0.41
Detector Quantum Efficiency	0.40	0.80
Cold Throughput	0.14	0.33
Net Throughput	0.05	0.14
Net Warm Emissivity	0.65	0.53
Net Detected Emissivity	0.09	0.17
SNR(10 zodi, 1 hr, $\Delta\lambda = 3$ μm)	19	44
SNR(1 zodi, 4 hr, $\Delta\lambda = 3$ μm)	4	9

5. Conclusions

As can be seen from Table 1, the Keck Interferometer's broadband detection limit, as set by random noise, should be on the order of 1 zodi in 1 observing track. The foreseen SNR thus also allows room for low-resolution spectroscopy to about the 10 zodi level. On the other hand, it is likely that systematic effects will be significant, especially in the early setup phase. The shorter wavelengths especially will tend to be more limited by systematics such as stellar light leakage due to imperfect nulls (Fig. 3), while the longer wavelengths are more likely to be purely background noise limited (Fig. 4).

Acknowledgments. The research described herein was carried out at the Jet Propulsion Laboratory, under a contract with NASA.

References

Angel 1998, R., in Exozodiacal Dust Workshop, NASA/CP 1998-10155, eds. D.E. Backman, L.J. Caroff, S.A. Sanford & D.H. Wooden, p. 209

Beichman, C.A., Woolf, N.J. & Lindensmith, C.A. 1999, Terrestrial Planet Finder, JPL publ. 99-3

Shao, M. & Colavita, M.M. 1992, ARA&A30, 457

Traub, W.A., Carleton, N.P., & Angel, J.R.P. 1996, in Science with the VLT Interferometer, ed. F. Paresce, Springer, p. 80

Woolf, N. & Angel, J.R.P. 1998, ARA&A36, 507